Published in final edited form as:

Nat Catal. 2023 March ; 6(3): 244–253. doi:10.1038/s41929-023-00925-4.

Elucidating electron-transfer events in polypyridine nickel complexes for reductive coupling reactions

Craig S. Day[1,2], **Ángel Rentería-Gómez**[3,5], **Stephanie J. Ton**[1,5], **Achyut Ranjan Gogoi**[3,5], **Osvaldo Gutierrez**[3,✉], **Ruben Martin**[1,2,4,✉]

[1]Institute of Chemical Research of Catalonia (ICIQ), The Barcelona Institute of Science and Technology, Tarragona, Spain.

[2]Departament de Química Analítica i Química Orgànica, Universitat Rovira i Virgili, Tarragona, Spain.

[3]Department of Chemistry, Texas A&M University, College Station, TX, USA.

[4]ICREA, Barcelona, Spain.

[5]These authors contributed equally: Ángel Rentería-Gómez, Stephanie J. Ton, Achyut Ranjan Gogoi.

Abstract

Polypyridine-ligated nickel complexes are widely used as privileged catalysts in a variety of cross-coupling reactions. The rapid adoption of these complexes is tentatively attributed to their ability to shuttle between different oxidation states and engage in electron-transfer reactions. However, these reactions are poorly understood in mechanistic terms. Here we investigate the reactivity of pseudohalide- and halide-ligated Ni(II) complexes, containing polypyridine ligands, in electron-transfer reactions. Specifically, Ni(II) halide complexes trigger comproportionation with Ni(0) with exceptional ease en route to Ni(I)L_n species, whereas the corresponding Ni(II) pseudohalide congeners are resistant to electron transfer, with Ni(I) pseudohalides being prone to disproportionation events. These observations are corroborated by electrochemical techniques and detailed quantum mechanical calculations. We also show that catalytically inactive Ni(II) pseudohalide complexes can be reactivated in the presence of exogeneous salts. From a broader perspective, this study provides rationalizations for overlooked and fundamental steps within the Ni-catalysed cross-coupling arena, thus offering blueprints for designing future Ni-catalysed reactions.

✉**Correspondence and requests for materials** should be addressed to Osvaldo Gutierrez or Ruben Martin. og.labs@tamu.edu; rmartinromo@iciq.es.

Author contributions

C.S.D. conceived the project. C.S.D. designed and performed the experimental studies unless otherwise stated. S.J.T. performed parts of the electrochemical experiments, stochiometric reductions and catalytic reactions. A.R.-G. and A.R.G. performed the computational studies. O.G. supervised the computational research. R.M. supervised the experimental research. C.S.D and R.M. prepared the initial manuscript. All authors contributed to discussions, commented on and edited the manuscript.

Competing interests

The authors declare no competing interests.

Supplementary information The online version contains supplementary material available at https://doi.org/10.1038/s41929-023-00925-4.

Recent years have witnessed the development of a myriad of Ni-catalysed reactions supported by polypyridine ligands as a new vehicle to forge sp^2 or sp^3 C–C(heteroatom) architectures. Unlike related studies based on phosphine (PR_3) or N-heterocyclic carbene ligands, the exceptional ability of nickel complexes bearing polypyridine ligands to shuttle between odd and even oxidation states–including the merger of both in dual catalytic processes–represents a key contributory factor for their rapid adoption in both academic and industrial work[1–5]. Despite the advances realized, progress in Ni-catalysed reactions with polypyridine ligands is mainly based on empirical discoveries; indeed, these processes remain poorly understood in mechanistic terms, thus limiting innovation in this field of expertise. This observation is likely to be due to the fleeting nature of the intermediate nickel species, the ambiguity behind the exact role exerted by the polypyridine backbone and the inherent propensity for alternative, yet undesired, bimolecular pathways. A close inspection of the literature data tacitly indicates that electron-transfer events between nickel species in either comproportionation, disproportionation or reduction events supported by polypyridine backbones are poorly understood. This is somewhat surprising given that nearly all Ni-catalysed reactions based on polypyridine ligands are proposed to undergo redox changes at some stage within the catalytic cycle, thus reinforcing the notion that electron-transfer events might have a critical role in either speciation and/or catalytic turnover (Fig. 1a). Such lack of mechanistic information results in arduous screening efforts for successful reaction development, as it is difficult to substantiate or differentiate between additives that are beneficial or poisonous to productive Ni catalysis. Indeed, there is ample consensus that Ni-catalysed reactions with poor control over the speciation contribute to high catalyst loadings, low reaction rates and low catalytic turnovers, probably due to a reasonable uncertainty of the oxidation state at the nickel centre, an insufficient concentration of the key on-cycle species and the formation of unproductive off-cycle intermediates[6–10]. Investigations by our group have recently shown that catalytic C–O bond-functionalization reactions follow on-cycle Ni(II)/Ni(0) cycles with phosphine ancillary ligands, where generation of Ni(I) species significantly hinders catalysis[11,12]. However, note that the formation of Ni(I) complexes has been proven to be essential to promote catalytic carboxylation reactions with well-defined Ni(I) alkyl complexes containing polypyridine ligands, thus showing the subtleties exerted by the nature of the ligand backbone on reactivity[13].

Early organometallic studies dating back to the 1960s showed that comproportionation or disproportionation could be controlled by the ligand backbone, with σ-donating triphenylphosphine (PPh_3) ligands promoting comproportionation reactions and π-accepting triphenyl phosphite ($P(OPh)_3$) ligands favouring disproportionation reactions (Fig. 1b)[14–18]. However, in general, comproportionation reactions are favoured for Ni(II) halide complexes bearing differently substituted ligand backbones (Fig. 1c)[8,14,15,17,19,20]. The dichotomy exerted by the ligand backbone on catalysis has also been recognized by others in elegant work, highlighting the importance that the nickel speciation might have on reactivity by populating Ni(0), Ni(I), Ni(II), or even Ni(III) manifolds[6–10,21–25]. However, a close look at the literature data reveals that unravelling the mechanistic intricacies of catalytic cross-coupling reactions containing polypyridine Ni complexes represents a notoriously challenging task[1,2,13,26–28]. This is likely to be due to the apparent propensity of the latter to participate in one- or two-electron pathways with equal ease and the

intermediacy of paramagnetic Ni(I) species and/or X-band electron paramagnetic resonance (EPR)-silent Ni(II) complexes. While elegant studies have demonstrated that polypyridyl **L**Ni(I) and **L**$_2$Ni(0) species can be accessed by either comproportionation or direct reduction with metallic reductants[10,13,26,27,29–32], there still exists a lack of empirical evidence on disproportionation reactions[28]; indeed, speculation remains on how disproportionation, comproportionation and reduction are interconnected with polypyridine nickel complexes, an aspect of utmost relevance when designing future Ni-catalysed reactions operating via redox-transfer processes (Fig. 1b). In addition, further ambiguity exists surrounding the tendency of nickel pseudohalide complexes to share the same reactivity trends as the corresponding nickel halide species. Such an observation can hardly be underestimated given the recent popularity of C–O electrophiles as powerful alternatives to organic halides in the cross-coupling arena[33–36], the enigmatic role that pseudohalide additives or base-sensitive functional groups such as alkoxides or carboxylates have in a wide variety of Ni-catalysed reactions of organic halides[37–39] and the existence of Ni pseudohalide complexes as on-cycle intermediates in catalytic processes, including carboxylation reactions and reductive coupling techniques[40–42]. Putting all these observations into perspective, we anticipated that this ambiguity limits the full potential of Ni-catalysed reactions to maintain the propagating on-cycle intermediates while preventing the formation of alternative off-cycle species. Driven by these observations, together with the popularity exerted by polypyridine nickel complexes in medicinal chemistry programmes and their unique ability to facilitate redox processes, it was deemed necessary to study in detail the intricacies of electron-transfer events at the molecular level as it may provide the basis for future developments in the Ni-catalysed arena.

In this Article, we describe a combined experimental and computational study aimed at unravelling the fundamental factors contributing to electron-transfer events in comproportionation, disproportionation and/or reduction reactions that occur between well-defined polypyridine Ni(II), Ni(I) and Ni(0) complexes. Stochiometric comproportionation and disproportionation reactions of polypyridine-bound Ni(II) complexes reveal that complexes bearing halide ligands (Cl, Br) react via comproportionation while those bearing pseudohalide ligands (pivalate, benzoate, phenoxide) undergo spontaneous disproportionation. These findings are further supported by cyclic voltammetry studies and computational studies, which show that halide ligands stabilize the respective Ni(I) species through decreasing the spin density via π-back-donation compared to their pseudohalide counterparts. This in turn promotes comproportionation for halide-bearing complexes and disproportionation for pseudohalide-bearing complexes. We further show that reduction of Ni(II) halide complexes to Ni(0) readily occurs while their pseudohalide analogues are unreactive in reductive coupling reactions using Zn or Mn and that exogenous salt additives restore reduction to Ni(0). The implications of these findings are further extended to catalytic cross-electrophile coupling reactions in which blueprints for appropriate precatalyst and additive selection are described.

Results

Identification of model ligand systems

We began our investigations by synthesizing a series of (**L**)$NiCl_2$ complexes containing either 1,10-phenanthroline (**L1**) or 2,2′-bipyridine (**L2**), the simplest ligands in the polypyridine series. It quickly became apparent that these complexes were not particularly soluble in conventional organic solvents (Fig. 2a). In addition, these species showed an inherent propensity to form mixtures of higher-order ligated nickel complexes of type $(\mathbf{L})_nNiCl_2$ (n = 0,1,2,3) or nickelate species such as $[(\mathbf{L})_3Ni][NiCl_4]$ (ref.[43]) thus reinforcing the need to utilize a different ligand backbone (Fig. 2b). Taking these observations into consideration, we focused our attention on 1,10-phenanthrolines with substituents at the 2 and 9′ positions. The choice of these ligands is certainly not arbitrary given their rapid adoption in a myriad of Ni-catalysed site-selective cross-coupling reactions where success seems to be intimately attributed to the inclusion of such a substitution pattern at the polypyridine backbone (Fig. 2c). In sharp contrast to **L1** and **L2**, single (**L**)$NiCl_2$ species were invariably obtained for both neocuproine (**L3**) and bathocuproine (**L4**), thus indirectly highlighting the intriguing role that the substitution pattern on the ligand might have in the speciation within the catalytic cycle. The molecular structure of (**L4**)$NiBr_2$ in the presence of additional **L4** was characterized by X-ray crystallography, showing that the Ni atom is in a canonical tetrahedral geometry[44]. While (**L3**)NiX_2 (X = Cl, Br) turned out to be insoluble in conventional solvents (**L4**)$NiCl_2$ showed an improved solubility and well-defined speciation. In line with this notion, no change in the paramagnetic ^{1}H NMR or UV-vis spectra was observed upon exposure of (**L4**)$NiCl_2$ to excess amounts of **L4**, thus confirming both that (**L4**)$NiCl_2$ exists as a single species and that these complexes meet the criteria for a well-behaved model system for studying redox-transfer events with catalytically relevant species (Fig. 2d).

Studying comproportionation and disproportionation

Aiming at investigating in detail electron transfer in polypyridyl nickel species, a representative set of (**L4**)NiX_2 complexes was synthesized by systematically varying the corresponding anionic ligand, with the corresponding Ni(II) alkoxide complexes being easily within reach upon exposure of the Ni(II) halide analogues to either KOPiv, $PhCO_2K$ or NaOPh (Fig. 3a). Interestingly, attempts at accessing Ni(II) alkoxide complexes by reacting LiO^tBu with (**L4**)$NiCl_2$ resulted in LiO^tBu Ni clusters of the formal composition $[NiLi_3Cl_2(O^tBu)_3]_2{\cdot}4THF$ with loss of **L4**, thus showing the influence that the alkoxide residue might have on Ni speciation (for X-ray diffraction see Supplementary Fig. 68). As expected, comproportionation between (**L4**)NiX_2 (X = Cl (**3a-Cl**), Br (**3a-Br**)) and (**L4**)Ni(COD) (COD = cyclooctadiene) provided a rapid and reliable access to well-defined Ni(I) halide complexes $[(\mathbf{L4})_2Ni^I]$ X (X = Cl (**4a-Cl**), Br (**4a-Br**)), in which **4a-Br** could be unambiguously determined by X-ray crystallography (Fig. 3b). Kinetic studies by UV-vis spectroscopy showed that the reaction occurred within seconds (Supplementary Fig. 14), consistent with rapid electron transfer where **5a** formally acts as a reductant and **3a-Cl/Br** acts as an oxidant to form stable Ni(I) species **4a-Cl/Br**. Interestingly, a strikingly different reactivity trend was observed for (**L4**)$Ni(OR)_2$ complexes (**3b**, R = Ph; **3c**, R = COPh; **3d**, R = Piv). Indeed, none of these complexes underwent reaction with $(\mathbf{L4})_2$Ni(0) as judged

by both EPR spectroscopy and paramagnetic ^{1}H NMR, thus ruling out the intervention of Ni(I) species (Supplementary Figs. 1–8). To validate whether these results were specific to **L4** or not, we synthesized (**L3**)Ni(OPiv)$_2$ (**3e**), the structure of which was determined by X-ray diffraction. In line with our expectations, no reaction was observed upon exposure of **3e** to (**L3**)$_2$Ni (**5b**), thus contributing to the perception that the nature of the halide backbone exerts a much more profound impact on both speciation and reactivity than initially anticipated.

Taking into consideration that reactions between Ni(0) and Ni(II) formally constitute electron-transfer events, it is reasonable to assume that they are under thermodynamic control. Therefore, if comproportionation between Ni(0) and Ni(II) carboxylate complexes does not occur, we tentatively speculated that the principle of microscopic reversibility should apply and disproportionation of Ni(I) alkoxides en route to both Ni(0) and Ni(II) should occur spontaneously. As shown in Fig. 3b, this hypothesis was indirectly confirmed by salt metathesis of **4a-Cl** with KOPiv. Interestingly, not even traces of (**L4**)Ni^{I}(OPiv) were observed by in situ monitoring of the reaction by EPR spectroscopy. Instead, formation of (**L4**)Ni(OPiv)$_2$ (**3d**) and (**L4**)$_2$Ni(0) was observed in quantitative yields, thus contributing to the perception that rapid disproportionation of transiently generated (**L4**)Ni^{I}(OPiv) comes into play. An otherwise identical outcome was obtained by either utilizing solvents with higher dielectric constants such as MeCN (ε = 37.5) or by replacing KOPiv with either PhCO$_2$K or NaOPh (Supplementary Figs. 15–22). These findings could be extended with Ni complexes containing **L3** instead, forming statistical mixtures of (**L3**)Ni(OPiv)$_2$ (**3d)** and (**L3**)$_2$Ni (**5b**) in quantitative yields upon reaction of [(**L3**)$_2$Ni] Cl (**4b-Cl**) with KOPiv.

Density functional theory studies on disproportionation and comproportionation

To gain insights into the distinct reactivity of nickel complexes and their ability to undergo comproportionation or disproportionation, we next turned to dispersion-corrected density functional theory (DFT) and domain-based local pair natural orbital coupled cluster method with single and double and perturbative triple excitations (DLPNO-CCSD(T)) calculations (Fig. 4 and see Supplementary Figs. 70–75 for additional information). First, we focused on the energy coordinate of comproportionation between (**L4**)$_2$Ni(0) (**5a**) and (**L4**)NiCl$_2$ (**3a-Cl**). As shown in Fig. 4a, an energetically viable pathway for comproportionation was found via ligand dissociation from (**L4**)$_2$Ni(0) (**5a**) and solvent (**L4**) NiCl$_2$ (**3a-Cl**) coordination en route to a bridging Ni(I) dimer (via ^{3}**TS1**) (see Supplementary Fig. 71 for full energy diagrams). In comparison to previously isolated [(dtbbpy)Ni(I)Cl]$_2$ dimeric species (dtbbpy = 4,4′-Di-tert-butyl-2,2′-dipyridyl), [(**L4**)Ni(I)Cl]$_2$ has longer Ni–Cl and Ni–Ni distances (2.41 versus ~2.33 Å and 3.35 versus 2.68 Å) presumably due to the increased steric effects associated with methyl substituents in the bathocuproine versus bipyridine scaffold[27]. The corresponding [(**L4**)Ni(I)Cl]$_2$ undergoes rapid dissociation (~2 kcal mol^{-1} barrier) to form the more thermodynamically favourable **L4**Ni(I)Cl monomeric species. In line with our experimental findings, comproportionation of all Ni(II) pseudohalide series was computed to be thermodynamically disfavoured by 6–8 kcal mol^{-1} (Fig. 4b). Despite exhaustive attempts we were not able to identify the comproportionation transition state (akin to **TS1**) for pseudohalide analogues. Nonetheless, these results strongly suggest that even if the barrier to undergo comproportionation is low, monomeric Ni(I) pseudohalide

complexes might favour the reverse disproportionation pathway (Supplementary Fig. 72). Presumably, halide ligands decrease the spin density (via π-back-donation)[45] of the monomeric LNi(I)X complexes that, in turn, stabilizes these species when compared to their parent Ni(II) and Ni(0) precursors[45]. This hypothesis was assessed by examining a range of pseudohalide ligands computationally (see Supplementary Fig. 74 for details). Interestingly, calculations revealed that subtle modulation of the electron properties of the pseudohalide ligand could decrease the electron density at the metal centre, thus making comproportionation thermodynamically favourable (Supplementary Figs. 74 and 75). These findings are particularly important, as they might lead to the foundation of methods for rational modulation of nickel complexes to control comproportionation and disproportionation pathways.

Electrochemical and stochiometric investigations

Having identified a strikingly divergent reactivity depending on the anionic ligand at Ni(II) and Ni(I) centres, we wondered whether these electron-transfer events could be indirectly assessed by comparing the cyclic voltammograms (CVs) of Ni(II) halide complexes to their corresponding Ni(II) carboxylate analogues. As shown in Fig. 5a, this turned out to be the case. Specifically, the CVs of (**L4**)$NiCl_2$ (**3a-Cl**) and (**L4**)$NiBr_2$ (**3a-Br**) resulted in two distinct, separated redox potentials of the Ni(II)/Ni(I) (Cl = −0.86 V, Br = −0.71 V versus saturated calomel electrode (SCE) in MeCN) and Ni(I)/Ni(0) (Cl = −1.24 V, Br = −1.10 V versus SCE in MeCN) couple. The separation of redox potentials and oxidation states is consistent with the ability to generate stable Ni(I) oxidation states, thus confirming that electron transfer and comproportionation between (**L4**)NiX_2 and $(\mathbf{L4})_2$Ni is particularly downhill. In striking contrast, the CV of (**L4**)$Ni(OPiv)_2$ (**3d**) revealed that only two electron redox events occur, in which Ni(II) is directly reduced to Ni(0) ($E_{p/2}$ = −1.43 V versus SCE in MeCN; $E_{p/2}$ = half-peak potential). The lack of stable (**L4**)Ni(I) carboxylate complexes is consistent with our stoichiometric experiments that showed no formation of (**L4**)Ni(OPiv) by either disproportionation of [$(\mathbf{L4})_2$Ni] Cl (**4a-Cl**) with KOPiv or comproportionation between $(\mathbf{L4})_2$Ni and (**L4**)$Ni(OPiv)_2$ (**3d**).

Given that a myriad of Ni-catalysed cross-electrophile couplings or reductive coupling reactions are commonly conducted with Mn or Zn as single-electron transfer reductants, we wondered whether the striking difference in redox potentials of Ni(II) halide and Ni(II) carboxylate complexes could be translated into a different reactivity profile in the presence of metallic reductants. According to the CVs of both $ZnCl_2$ ($E_{p/2}$ = −1.26 V versus SCE in MeCN) and $MnCl_2$ ($E_{p/2}$ = −1.38 V versus SCE in MeCN), we anticipated that Mn and Zn would be competent for triggering single-electron transfer reduction of (**L4**)Ni(II) halides en route to Ni(I) and subsequently to Ni(0); however, it was unclear whether (**L4**)$Ni(OPiv)_2$ (**3d**) would be reduced due to its similar redox potential with either Mn or Zn (Fig. 5a). This hypothesis was corroborated by stoichiometric reduction of (**L4**)$NiBr_2$ (**3a-Br**) with Zn or Mn in the presence of excess amounts of **L4** to stabilize low-coordinate Ni species and bind Zn(II) or Mn(II) salts obtained after single-electron transfer. As anticipated $(\mathbf{L4})_2$Ni was obtained equally well by using either Mn or Zn (Fig. 5b). In sharp contrast, no reaction was observed upon simple exposure of (**L4**)$Ni(OPiv)_2$ (**3d**) to Mn or Zn; the starting Ni(II) precursor was recovered unaltered. These results indirectly suggested that

formation of (**L**)Ni(OR)$_2$ in Ni-catalysed reactions of C–O electrophiles or organic halides requiring pseudohalide bases operating via single-electron transfer might be particularly problematic for catalytic turnover. However, we speculated that addition of inorganic halide salts such as LiBr or $ZnBr_2$ might be beneficial for turnover by generating (**L4**) NiX_2 in situ (X = halide). This hypothesis was indirectly corroborated by stoichiometric studies that showed clean formation of (**L4**)$NiBr_2$ (**3a**-**Br**) upon exposure of (**L4**)Ni(OPiv)$_2$ (**3d**) to LiBr and quantitative formation of (**L4**)$_2$Ni(0) (**5a**) by reduction of (**L4**)Ni(OPiv)$_2$ (**3d**) with Zn in the presence of $ZnBr_2$ or in 80% yield with LiBr. These results can hardly be underestimated, as they highlight the non-negligible impact that a priori innocent inorganic salts might have in aiding reduction events when Ni(II) pseudohalide complexes are formed during catalytic reactions. Although these findings allow the enigmatic, yet beneficial, role exerted by exogenous halide salts in a series of recent Ni-catalysed reductive coupling reactions of C–O electrophiles to be rationalized, it was unclear whether the inclusion of Zn(II) salts might populate other conceivable pathways. Indeed, recent findings from our group showed the formation of unorthodox Ni/Zn clusters via single-electron transfer and ligand-sequestering events when combining well-defined Ni(0) [PCy_3] (Cy = cyclohexyl) complexes with $ZnCl_2$ (ref.[11]). Interestingly, while no heterobimetallic Ni/Zn species were obtained upon exposure of (**L4**)$_2$Ni to $ZnCl_2$, we identified (**L4**)$ZnCl_2$ in the crude mixtures, thus suggesting an inevitable ligand-sequestering event between hard Ni(0) and Zn(II) centres. Although tentative, we believe this divergent reactivity is likely to originate from **L4** being a poor σ-donor ligand when compared to PCy_3, thus making the corresponding (**L4**)$_2$Ni complex a weaker reductant.

Relevance in nickel-catalysed cross-coupling reactions

Altogether, the results of Figs. 3–5 stand as a testament to the unique reactivity exerted by polypyridine nickel complexes in electron-transfer events and the relevance that these findings might have in Ni-catalysed cross-coupling reactions. Most apparent is the non-negligible influence that commonly employed pseudohalide bases and/or additives might have in catalyst speciation, inhibiting reduction from **L**Ni(II) (pseudohalides) while preventing formation of Ni(I) species via disproportionation reactions. Driven by this perception, we turned our attention to unravel the implications that these findings might have in Ni-catalysed reductive coupling reactions operating via the intermediacy of Ni(I) complexes. The deleterious effect that pseudohalide bases have on Ni-catalysed reductive couplings was apparent by the inclusion of KOPiv after 60 minutes in the cross-electrophile coupling of alkyl bromides and aryl bromides reported by Yin based on the Ni/**L4** couple (Fig. 6a–teal trace)[46]. As shown in Fig. 6a, a significant reduction in both reaction rate and yield was observed when compared to the standard reaction, suggesting the formation of inactive (**L4**)Ni(OPiv)$_2$ species (**3d**). The latter observation was corroborated by matrix-assisted laser desorption/ionization mass spectrometry (MALDI-MS) of the crude mixture, resulting in a rather distinctive m/z pattern for **3d** (Supplementary Fig. 36). As expected, no reaction was observed when utilizing solely **3d** as the precatalyst whereas catalytic activity was significantly restored upon addition of nBu$_4$NBr after 90 minutes (Fig. 6a–grey trace). However, note that a lower rate was found when compared to that of the standard reaction using the NiI_2/**L4** couple due to the presence of pivalate anions. Similar findings were observed when studying the site-selective Ni-catalysed carboxylation of allylic alcohols

with CO_2 (1 atm) based on a Ni/**L4** regime and Zn as metallic reductant, where addition of $MgCl_2$ was found to be critical for success (Fig. 6b)[40]. In line with our expectations, removal of $MgCl_2$ resulted in a significant loss in efficiency (15% yield). It is likely that the minor quantities of **8** formed under these conditions can be attributed to the formation of $ZnBr_2$ upon reduction of $NiBr_2$, allowing the formation of (**L4**)$NiBr_2$ (**3a-Br**) upon reaction of (**L4**)Ni pseudohalides with $ZnBr_2$. This observation was indirectly corroborated by the lack of reaction found when utilizing $Ni(COD)_2$ as the precatalyst in the absence of either $ZnBr_2$ or $MgCl_2$ whereas reactivity was restored upon addition of the latter, resulting in 61% yield of **8**. Similarly, a catalytic system based on **3a** without $MgCl_2$ resulted in no formation of **8**. Extending these findings to ligand systems beyond **L4** that form Ni carboxylate species on-cycle, we studied the reductive carboxylation of dienes employing 2-methyl-4,7-diphenyl-1,10-phenanthroline (**L5**) and bathrophenanthroline (**L6**). We found similar reactivity to that observed in the allylic carboxylation in which $Ni(COD)_2$ without a halide source resulted in no carboxylated product, but reactivity could be restored upon adding inorganic halide source $n$$Bu_4NBr$ (Supplementary Fig. 39)[47]. Interested in the possibility that these results may extend to other ligand systems we first compared the CVs of bipyridine-ligated nickel complexes (**L2**) $NiBr_2$ and (**L2**)$Ni(OPiv)_2$ (Supplementary Figs. 52 and 53)[48]. Supporting the notion that the investigations with **L4** could be extended to **L2** were the similar CVs between the analogous complexes, with (**L2**) $NiBr_2$ displaying distinct Ni(II/I) and Ni(I/0) redox waves while (**L2**) $Ni(OPiv)_2$ displayed a single Ni(II/0) redox wave. Turning to study the generality of these findings and the impact of forming other on-cycle pseudohalide species, we considered the reductive coupling of alkyl tosylates with aryl bromides[35]. Consistent with the previous findings, removal of KI from the standard conditions resulted in a significant drop in yield (Fig. 6c entries 1 and 2). Likewise, employing halide-free precatalyst $Ni(COD)_2$ was less effective than the standard conditions but performing the reaction with $Ni(COD)_2$ and removing KI resulted in trace product (5%). Putting all these findings into perspective, we believe these experiments do not only provide a rational explanation of the enigmatic role exerted by additives in existing Ni-catalysed reductive couplings but also offer a gateway for designing future Ni-catalysed reactions.

Conclusions

In summary, this work uncovers the enigmatic role exerted by anionic ligands in electron-transfer events occurring in comproportionation, disproportionation and reduction reactions of polypyridine nickel complexes, elementary steps commonly encountered in the Ni-catalysed cross-coupling arena. Specifically, stoichiometric and quantum mechanical studies tacitly reveal that Ni(II) halides easily react by comproportionation with Ni(0) complexes to form Ni(I) species. In sharp contrast, Ni(II) pseudohalides are unreactive whereas their corresponding Ni(I) analogues react irreversibly by disproportionation. The implications of these findings are strongly related to the formation of off-cycle species that compromise catalytic turnover, thus leading to catalytic reactions with poor efficiency. Taking into consideration the popularity exerted by polypyridine nickel complexes in one- or two-electron pathways in a myriad of catalytic reactions and their rapid adoption in industrial work, our study provides long-awaited insights into mechanistic aspects of utmost relevance for designing future Ni-catalysed reactions.

Methods

General

Reactions were carried out under N_2 in a glovebox or on a Schlenk line unless otherwise noted. Reagents and solvents were purified by standard means. See Supplementary Methods for detailed conditions and the characterization data.

Synthesis of (L4)Ni(OPiv)$_2$

In the glovebox (**L4**)$NiCl_2$ (224 mg, 0.46 mmol) was added to a 12 ml vial, together with potassium pivalate (206 mg, 1.66 mmol). A stir bar was added and the vial was charged with 6 ml toluene. This turned the pink powder to a pink suspension and this was stirred overnight. After 16 h the resulting green solution was filtered through a Celite plug with the salt being filtered off and a green solution was collected. The solvent was then removed to afford a green solid and this was washed 3 times with pentane (1 ml) to give (**L4**)$Ni(OPiv)_2$ (199 mg, 70% yield) as a green powder.

Synthesis of (L4)Ni(OCOPh)$_2$

In the glovebox (**L4**)$NiCl_2$ (122 mg, 0.25 mmol) and potassium benzoate (83 mg, 0.52 mmol, 2.08 equiv.) were added to a 10 ml vial. A stir bar was added and the vial was then charged with 3 ml THF. The solution was stirred overnight, during which a colour change from pink to orange to green was observed. The solvent was then removed and the solid was dissolved in DCM. This mixture was filtered through a Celite plug where a white solid was filtered off. The green solution was concentrated to dryness. The solid was washed 3 times with pentane (3 ml) to afford (**L4**)$Ni(OCOPh)_2$ as a green powder (128 mg, 78% yield).

Synthesis of [(L4)Ni(OPh)$_2$]$_2$

In the glovebox (**L4**)$NiCl_2$ (158 mg, 0.32 mmol) and sodium phenoxide (116 mg, 1.00 mmol, 3.1 equiv.) were added to a 10 ml vial. A stir bar was added and the vial was then charged with 5 ml toluene and the solution was stirred overnight. The solvent was then removed and the residue was redissolved in DCM (sparingly soluble). This mixture was filtered through a Celite plug. The solvent was then removed and the solid was washed with 3 times with pentane (3 ml) to afford [(**L4**)$Ni(OPh)_2]_2$ as a brown powder (88 mg, 45 % yield).

Synthesis of [NiLi$_3$Cl$_2$(O^{t}Bu)$_3$]$_2$·4THF

In the glovebox (**L4**)$NiCl_2$ (113 mg, 0.23 mmol) and lithium *tert*-butoxide (41 mg, 0.51 mmol) were added to a 10 ml vial. A stir bar was added and the vial was charged with 3 ml THF and the solution was stirred overnight. The solvent was then removed and the residue was dissolved in minimal THF and this mixture was then filtered through a Celite plug. The solvent was then removed and the residue was washed 3 times with pentane (3 ml) to afford $[NiLi_3Cl_2(O^tBu)_3]_2$·4THF as a blue powder (88 mg, quantitative).

Supplementary Material

Refer to Web version on PubMed Central for supplementary material.

Acknowledgements

We thank ICIQ and FEDER/MCI−AEI/PGC2018-096839-B-I00 for financial support. C.S.D. thanks the European Union's Horizon 2020 under the Marie Curie PREBIST grant agreement 754558. S.J.T. thanks Marie Sklodowska-Curie grant agreement No. 859910. O.G. thanks the NIGMS NIH (R35GM137797), the Camille and Henry Dreyfus Foundation and the Welch Foundation (A-2102-20220331) for funding and Texas A&M University HPRC resources (https://hprc.tamu.edu) for computational resources. We sincerely thank T. Skrydstrup for allowing revisions to be completed using his laboratory space and equipment, J. Benet for X-ray crystallographic data and G. Stoica for assistance with EPR experiments.

Data availability

Experimental procedures and characterization data for the stochiometric experiments, catalysts and the synthesized compounds along with computational information are included in the Supplementary Information. Crystallographic data are available from the Cambridge Crystallographic Data Centre with the following codes: **3d** (CCDC-2175355), **3c** (CCDC-2175356), **3b** (CCDC-2175354), **4a-Br** (CCDC-2175353), **3a-Br** (CCDC-2175357), $[NiLi_3Cl_2(O^tBu)_3{\cdot}2THF]_2$ (CCDC-2175358) and **3e** (CCDC-2175352). Other data are available from the corresponding authors upon reasonable request.

References

1. Diccianni JB & Diao T Mechanisms of nickel-catalyzed cross-coupling reactions. Trends Chem. 1, 830–844 (2019).
2. Diccianni J, Lin Q & Diao T Mechanisms of nickel-catalyzed coupling reactions and applications in alkene functionalization. Acc. Chem. Res 53, 906–919 (2020). [PubMed: 32237734]
3. Tasker SZ, Standley EA & Jamison TF Recent advances in homogeneous nickel catalysis. Nature 509, 299–309 (2014). [PubMed: 24828188]
4. Hazari N, Melvin PR & Beromi MM Well-defined nickel and palladium precatalysts for cross-coupling. Nat. Rev. Chem 1, 0025 (2017). [PubMed: 29034333]
5. Everson DA & Weix DJ Cross-electrophile coupling: principles of reactivity and selectivity. J. Org. Chem 79, 4793–4798 (2014). [PubMed: 24820397]
6. Mohadjer Beromi M et al. Mechanistic study of an improved Ni precatalyst for Suzuki–Miyaura reactions of aryl sulfamates: understanding the role of Ni(I) species. J. Am. Chem. Soc 139, 922–936 (2017). [PubMed: 28009513]
7. Barth EL et al. Bis(dialkylphosphino)ferrocene-ligated nickel(II) precatalysts for Suzuki–Miyaura reactions of aryl carbonates. Organometallics 38, 3377–3387 (2019). [PubMed: 32565607]
8. Mohadjer Beromi M, Banerjee G, Brudvig GW, Hazari N & Mercado BQ Nickel(I) aryl species: synthesis, properties, and catalytic activity. ACS Catal. 8, 2526–2533 (2018). [PubMed: 30250755]
9. Mohadjer Beromi M et al. Modifications to the aryl group of dppf-ligated Ni σ-aryl precatalysts: impact on speciation and catalytic activity in Suzuki–Miyaura coupling reactions. Organometallics 37, 3943–3955 (2018). [PubMed: 31736532]
10. Yanagi T, Somerville RJ, Nogi K, Martin R & Yorimitsu H Ni-catalyzed carboxylation of $C(sp^2)$–S bonds with CO_2: evidence for the multifaceted role of Zn. ACS Catal. 10, 2117–2123 (2020).
11. Day CS, Somerville RJ & Martin R Deciphering the dichotomy exerted by Zn(II) in the catalytic sp^2 C–O bond functionalization of aryl esters at the molecular level. Nat. Catal 4, 124–133 (2021).
12. Somerville RJ, Hale LVA, Gómez-Bengoa E, Burés J & Martin R Intermediacy of Ni–Ni species in sp^2 C–O bond cleavage of aryl esters: relevance in catalytic C–Si bond formation. J. Am. Chem. Soc 140, 8771–8780 (2018). [PubMed: 29909614]
13. Somerville RJ et al. Ni(I)–alkyl complexes bearing phenanthroline ligands: experimental evidence for CO_2 insertion at Ni(I) centers. J. Am. Chem. Soc 142, 10936–10941 (2020). [PubMed: 32520556]

14. Heimbach P Changes in the coordination number of Ni(0) and Ni(I) compounds. Angew. Chem. Int. Ed 3, 648 (1964).
15. Tsou TT & Kochi JK Mechanism of oxidative addition. Reaction of nickel(0) complexes with aromatic halides. J. Am. Chem. Soc 101, 6319–6332 (1979).
16. Cundy CS & Nöth H Metal-boron compounds: XI. Complexes derived from reactions of bis(triphenylphosphine)(π-ethylene) nickel with alkyl and boron halides. J. Organomet. Chem 30, 135–143 (1971).
17. Porri L, Gallazzi MC & Vitulli G Complexes of nickel(I) with triphenylphosphine. Chem. Commun, 228–228 (1967).
18. Beattie DD, Lascoumettes G, Kennepohl P, Love JA & Schafer LL Disproportionation reactions of an organometallic Ni(I) amidate complex: scope and mechanistic Investigations. Organometallics 37, 1392–1399 (2018).
19. Dible BR, Sigman MS & Arif AM Oxygen-induced ligand dehydrogenation of a planar bis-μ-chloronickel(I) dimer featuring an NHC ligand. Inorg. Chem 44, 3774–3776 (2005). [PubMed: 15907100]
20. Schunn RA Preparation and reactions of triethylphosphine complexes of zerovalent nickel, palladium, and platinum. Inorg. Chem 15, 208–212 (1976).
21. Dürr AB, Fisher HC, Kalvet I, Truong K-N & Schoenebeck F Divergent reactivity of a dinuclear (NHC)nickel(I) catalyst versus nickel(0) enables chemoselective trifluoromethylselenolation. Angew. Chem. Int. Ed 56, 13431–13435 (2017).
22. Kalvet I, Guo Q, Tizzard GJ & Schoenebeck F When weaker can be tougher: the role of oxidation state (I) in P- vs N-ligand-derived Ni-catalyzed trifluoromethylthiolation of aryl halides. ACS Catal. 7, 2126–2132 (2017). [PubMed: 28286695]
23. Kapat A, Sperger T, Guven S & Schoenebeck F *E*-olefins through intramolecular radical relocation. Science 363, 391–396 (2019). [PubMed: 30679370]
24. Yuan M, Song Z, Badir SO, Molander GA & Gutierrez O On the nature of $C(sp^3)$–$C(sp^2)$ bond formation in nickel-catalyzed tertiary radical cross-couplings: a case study of Ni/photoredox catalytic cross-coupling of alkyl radicals and aryl halides. J. Am. Chem. Soc 142, 7225–7234 (2020). [PubMed: 32195579]
25. Phapale VB, Guisán-Ceinos M, Buñuel E & Cárdenas DJ Nickel-catalyzed cross-coupling of alkyl zinc halides for the formation of $C(sp^2)$—$C(sp^3)$ bonds: scope and mechanism. Chem. Eur. J 15, 12681–12688 (2009). [PubMed: 19847828]
26. Lin Q & Diao T Mechanism of Ni-catalyzed reductive 1,2-dicarbofunctionalization of alkenes. J. Am. Chem. Soc 141, 17937–17948 (2019). [PubMed: 31589820]
27. Mohadjer Beromi M, Brudvig GW, Hazari N, Lant HMC & Mercado BQ Synthesis and reactivity of paramagnetic nickel polypyridyl complexes relevant to $C(sp^2)$–$C(sp^3)$coupling reactions. Angew. Chem. Int. Ed 58, 6094–6098 (2019).
28. Ting SI, Williams WL & Doyle AG Oxidative addition of aryl halides to a Ni(I)-bipyridine complex. J. Am. Chem. Soc 144, 5575–5582 (2022). [PubMed: 35298885]
29. Till NA, Oh S, MacMillan DWC & Bird MJ The application of pulse radiolysis to the study of Ni(I) intermediates in Ni-catalyzed cross-coupling reactions. J. Am. Chem. Soc 143, 9332–9337 (2021). [PubMed: 34128676]
30. Ting SI et al. 3d-d Excited states of Ni(II) complexes relevant to photoredox catalysis: spectroscopic identification and mechanistic implications. J. Am. Chem. Soc 142, 5800–5810 (2020). [PubMed: 32150401]
31. Huang L, Ackerman LKG, Kang K, Parsons AM & Weix DJ LiCl-accelerated multimetallic cross-coupling of aryl chlorides with aryl triflates. J. Am. Chem. Soc 141, 10978–10983 (2019). [PubMed: 31257881]
32. Powers DC, Anderson BL & Nocera DG Two-electron HCl to H_2 photocycle promoted by Ni(II) polypyridyl halide complexes. J. Am. Chem. Soc 135, 18876–18883 (2013). [PubMed: 24245545]
33. Juliá-Hernández F, Moragas T, Cornella J & Martin R Remote carboxylation of halogenated aliphatic hydrocarbons with carbon dioxide. Nature 545, 84–88 (2017). [PubMed: 28470192]
34. Li Z et al. Electrochemically enabled, nickel-catalyzed dehydroxylative cross-coupling of alcohols with aryl halides. J. Am. Chem. Soc 143, 3536–3543 (2021). [PubMed: 33621464]

35. Molander GA, Traister KM & O'Neill BT Engaging nonaromatic, heterocyclic tosylates in reductive cross-coupling with aryl and heteroaryl bromides. J. Org. Chem 80, 2907–2911 (2015). [PubMed: 25711834]
36. Dong Z & Macmillan DWC Metallaphotoredox-enabled deoxygenative arylation of alcohols. Nature 598, 451–456 (2021). [PubMed: 34464959]
37. Zhang Y, Xu X & Zhu S Nickel-catalysed selective migratory hydrothiolation of alkenes and alkynes with thiols. Nat. Commun 10, 1752 (2019). [PubMed: 30988306]
38. Smith RT et al. Metallaphotoredox-catalyzed cross-electrophile Csp^3-Csp^3 coupling of aliphatic bromides. J. Am. Chem. Soc 140, 17433–17438 (2018). [PubMed: 30516995]
39. Peng L, Li Z & Yin G Photochemical nickel-catalyzed reductive migratory cross-coupling of alkyl bromides with aryl bromides. Org. Lett 20, 1880–1883 (2018). [PubMed: 29561162]
40. van Gemmeren M et al. Switchable site-selective catalytic carboxylation of allylic alcohols with CO_2. Angew. Chem. Int. Ed 56, 6558–6562 (2017).
41. Tortajada A, Börjesson M & Martin R Nickel-catalyzed reductive carboxylation and amidation reactions. Acc. Chem. Res 54, 3941–3952 (2021). [PubMed: 34586783]
42. Tortajada A, Juliá-Hernández F, Börjesson M, Moragas T & Martin R Transition-metal-catalyzed carboxylation reactions with carbon dioxide. Angew. Chem. Int. Ed 57, 15948–15982 (2018).
43. Harris CM & McKenzie ED Nitrogenous chelate complexes of transition metals–III: bis-chelate complexes of nickel (II) with 1,10-phenanthroline, 2,2′-bipyridyl and analogous ligands. J. Inorg. Nucl. Chem 29, 1047–1068 (1967).
44. Kinnunen T-JJ, Haukka M, Pakkanen TT & Pakkanen TA Four-coordinated bipyridine complexes of nickel for ethene polymerization–the role of ligand structure. J. Organomet. Chem 613, 257–262 (2000).
45. Fagnou K & Lautens M Halide effects in transition metal catalysis. Angew. Chem. Int. Ed 41, 26–47 (2002).
46. Peng L et al. Ligand-controlled nickel-catalyzed reductive relay cross-coupling of alkyl bromides and aryl bromides. ACS Catal. 8, 310–313 (2018).
47. Tortajada A, Ninokata R & Martin R Ni-catalyzed site-selective dicarboxylation of 1,3-dienes with CO_2. J. Am. Chem. Soc 140, 2050–2053 (2018). [PubMed: 29376353]
48. Eremenko IL et al. Bi- and mononuclear nickel(II) trimethylacetate complexes with pyridine bases as ligands. Inorg. Chem 38, 3764–3773 (1999).

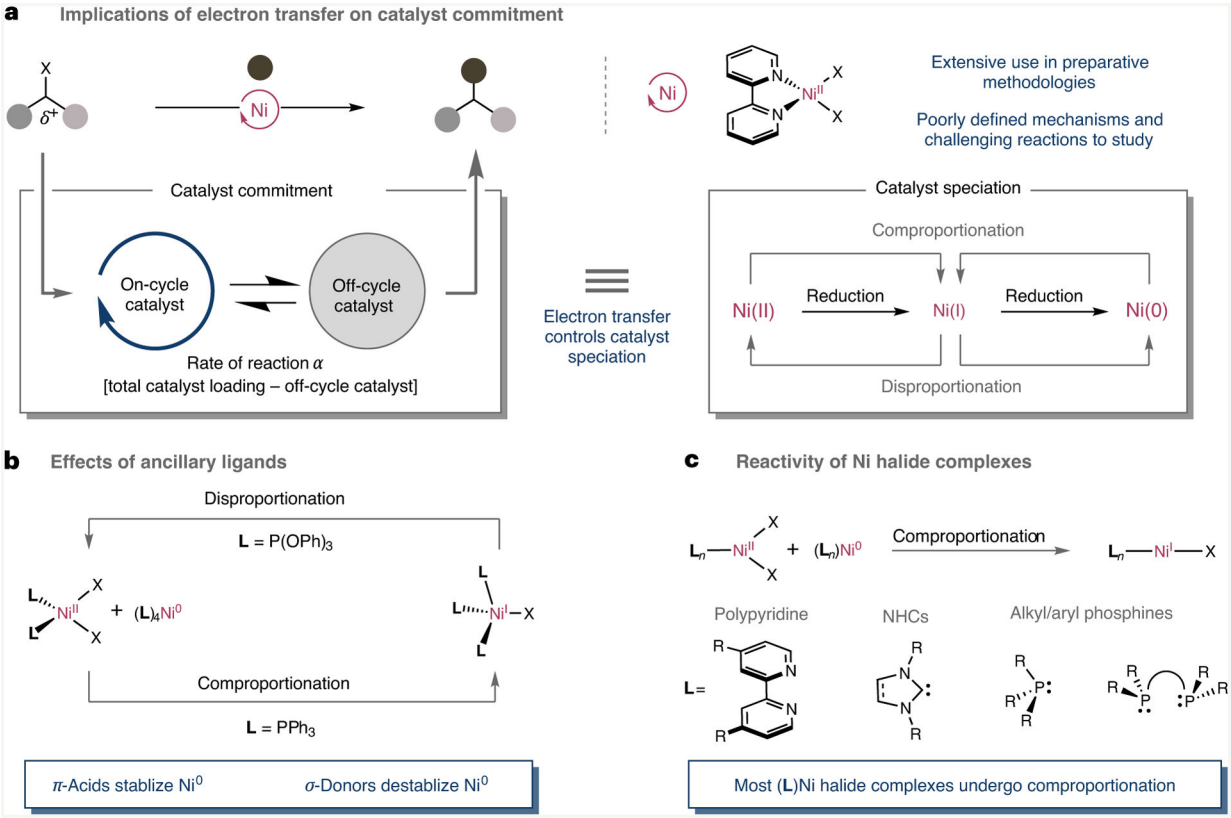

Fig. 1 |. Ambiguity in electron transfer.

a, Implications of electron transfer on the formation of on-cycle or off-cycle nickel complexes. **b**, Impact of ancillary ligands on disproportionation or comproportionation. **c**, Comproportionation of Ni(II) halides supported by ancillary ligands. NHCs, N-heterocyclic carbenes.

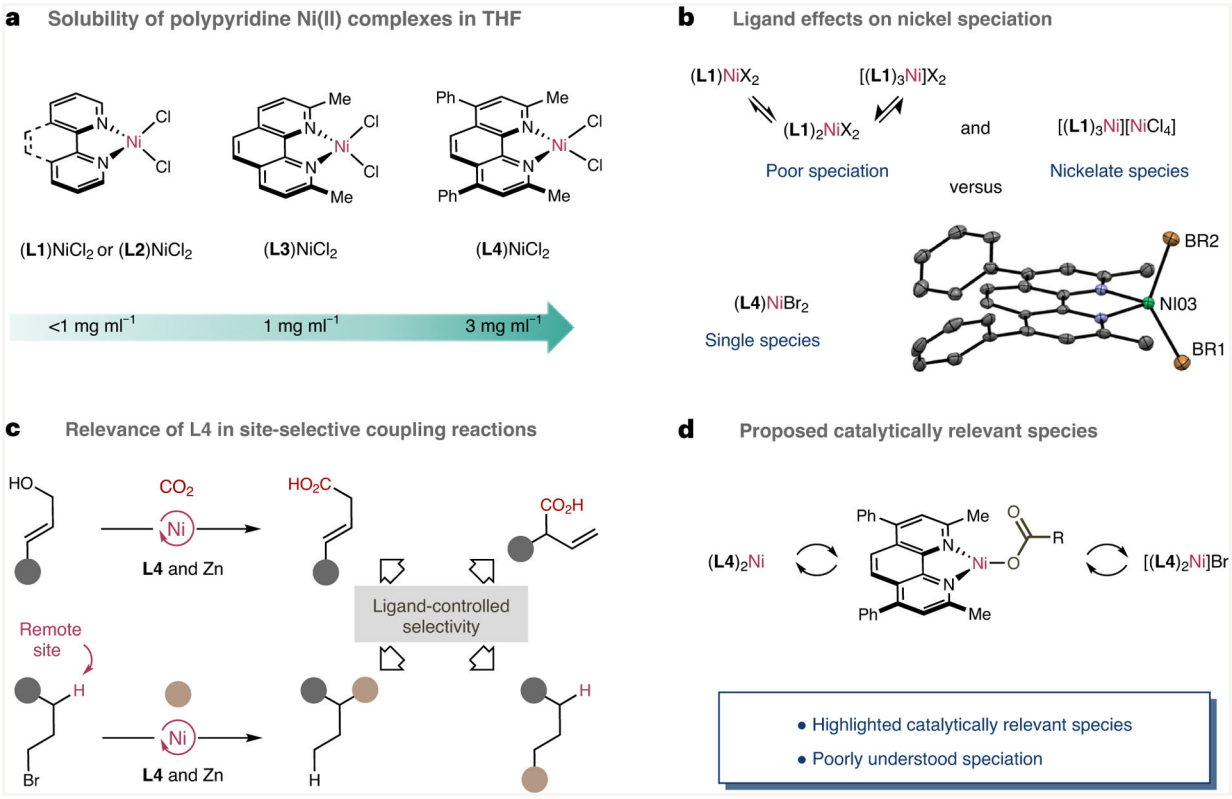

Fig. 2 |. Considerations for studying Ni polypyridine complexes.

a, Effect of ligand substitution on complex solubility. **b**, Ligand effects on nickel speciation. **c**, Relevance of **L4** in site-selective cross-coupling reactions. **d**, Catalytically relevant species in nickel-catalysed coupling reactions.

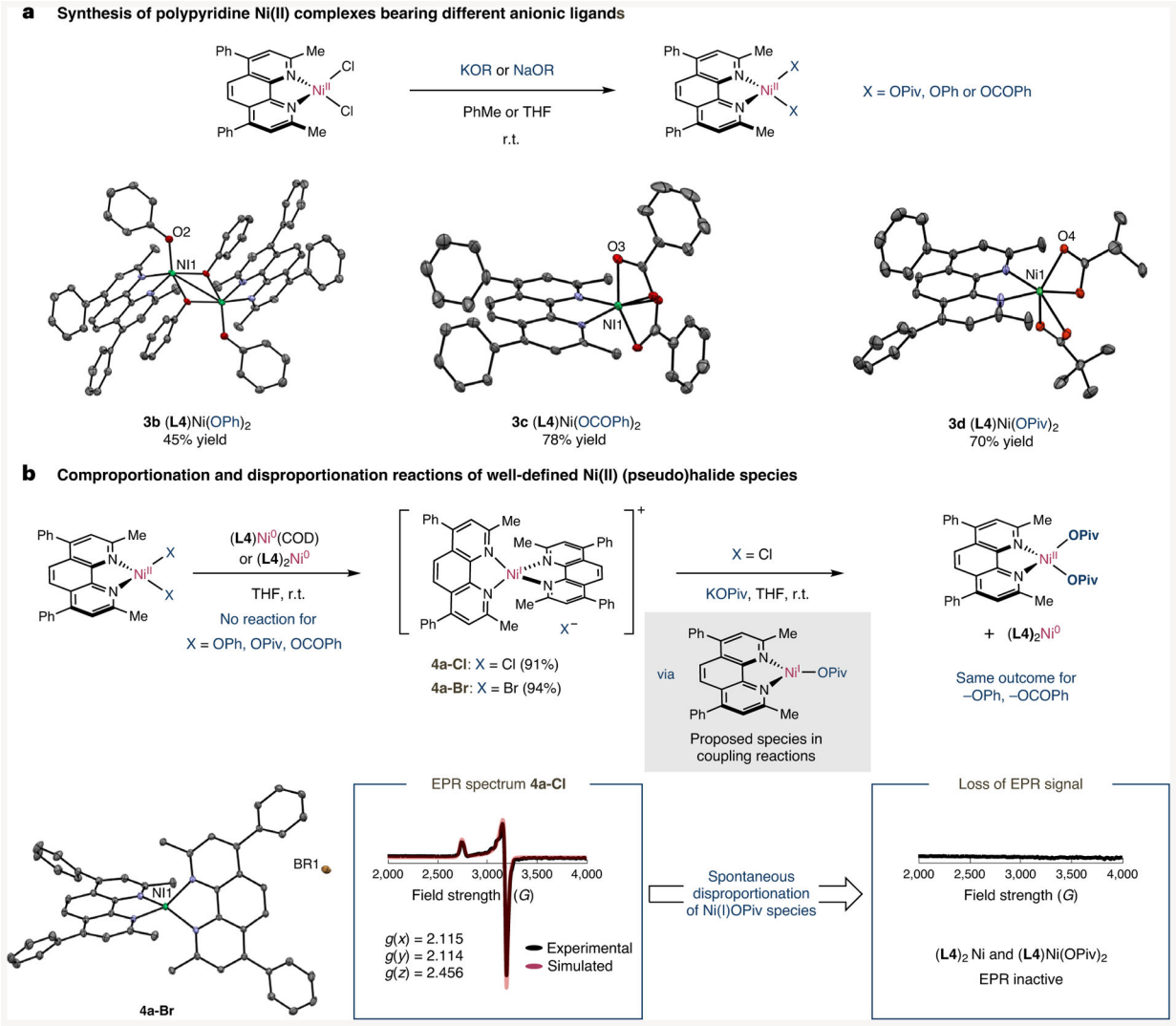

Fig. 3 |. Effect of anonic ligands on electron transfer.

a, Synthesis of Ni(II) pseudohalide complexes [KOPiv (3 equiv.), PhMe, 16 h, r.t.; PhCO2K (2 equiv.), THF, 16 h, r.t.; NaOPh (3 equiv.), PhMe, 16 h, r.t.]. **b**, Investigation of the nature of the anionic ligand on comproportionation and disproportionation. COD, cyclooctadiene; OPiv, pivalate; r.t., room temperature.

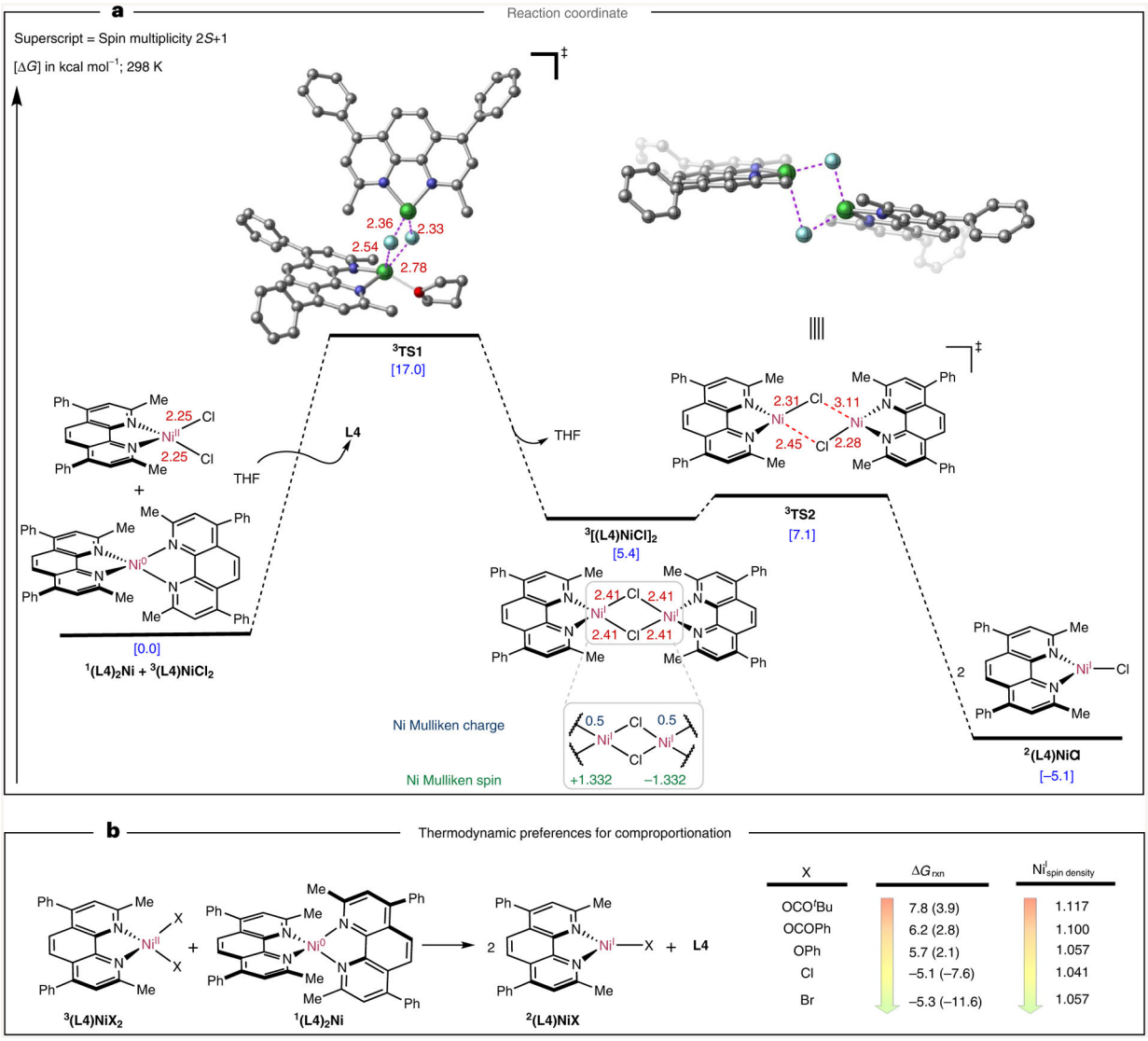

Fig. 4 |. Computational study of comproportionation.

a, Lowest energy pathway computed at the UB3LYP-D3/def2tzvpp-CPCM(THF)//UB3LYP-D3/def2svp-CPCM(THF) level for comproportionation of (**L4**)$_2$NiCl$_2$. **b**, Computed free energies for the formation of monomeric (**L4**)Ni(I)-X species from the corresponding Ni(II) and Ni(0) complexes calculated at the UB3LYP-D3/def2tzvpp-CPCM(THF)//UB3LYP-D3/def2svp-CPCM(THF) and DLPNO-CCSD(T)/def2svp-CPCM(THF)//UB3LYP-D3/def2svp-CPCM(THF) (in parenthesis) levels of theory.

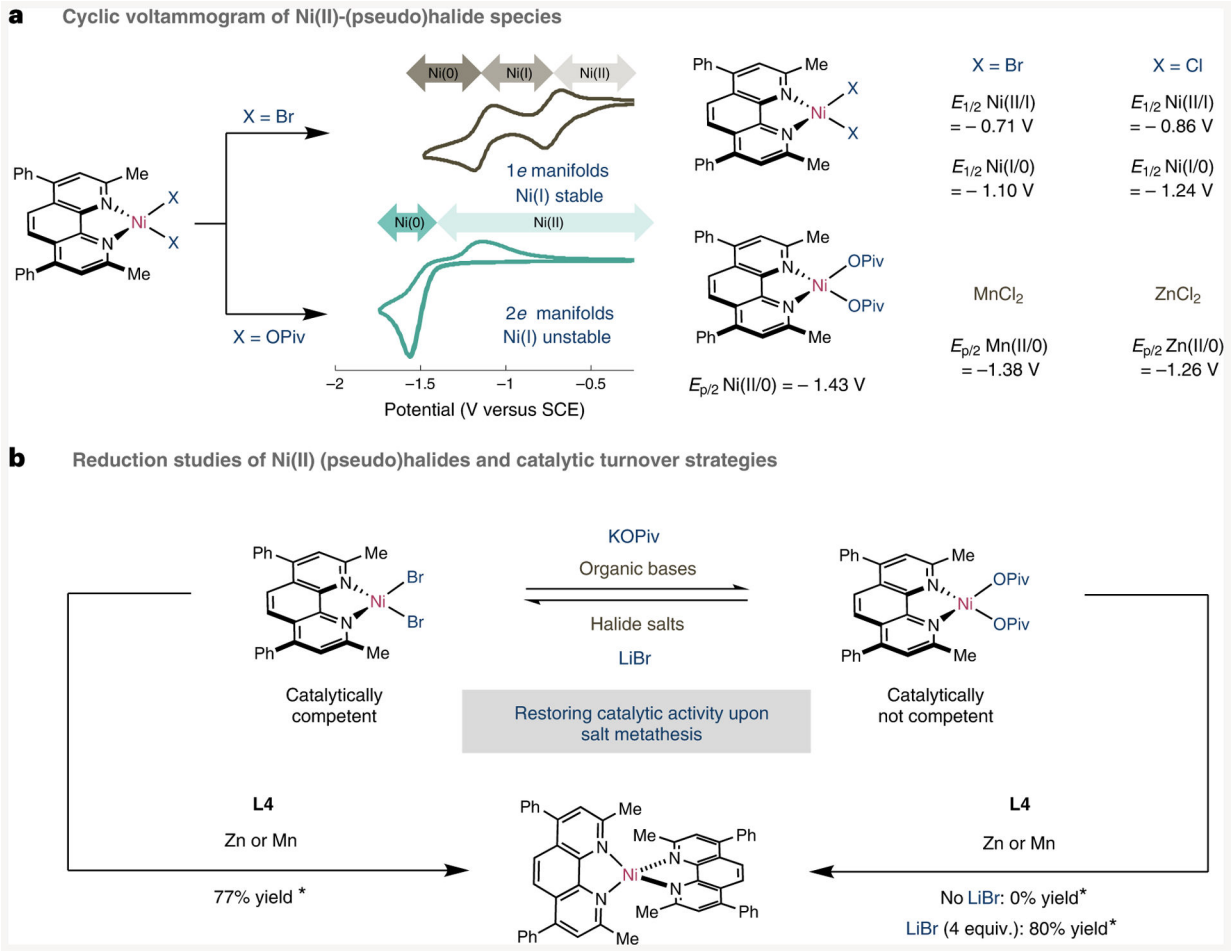

Fig. 5 |. Electrochemical studies and stoichiometric reduction studies.

a, CVs of (**L4**)$NiBr_2$ and (**L4**)$Ni(OPiv)_2$ and comparison of redox potentials. **b**, Implications of halide exchange on reduction. *Additional **L4** added to stabilize (**L4**)$_2$Ni. SCE, saturated calomel electrode. $E_{1/2}$ = half-wave potential; $E_{p/2}$ = half-peak potential; OPiv = Pivalate.

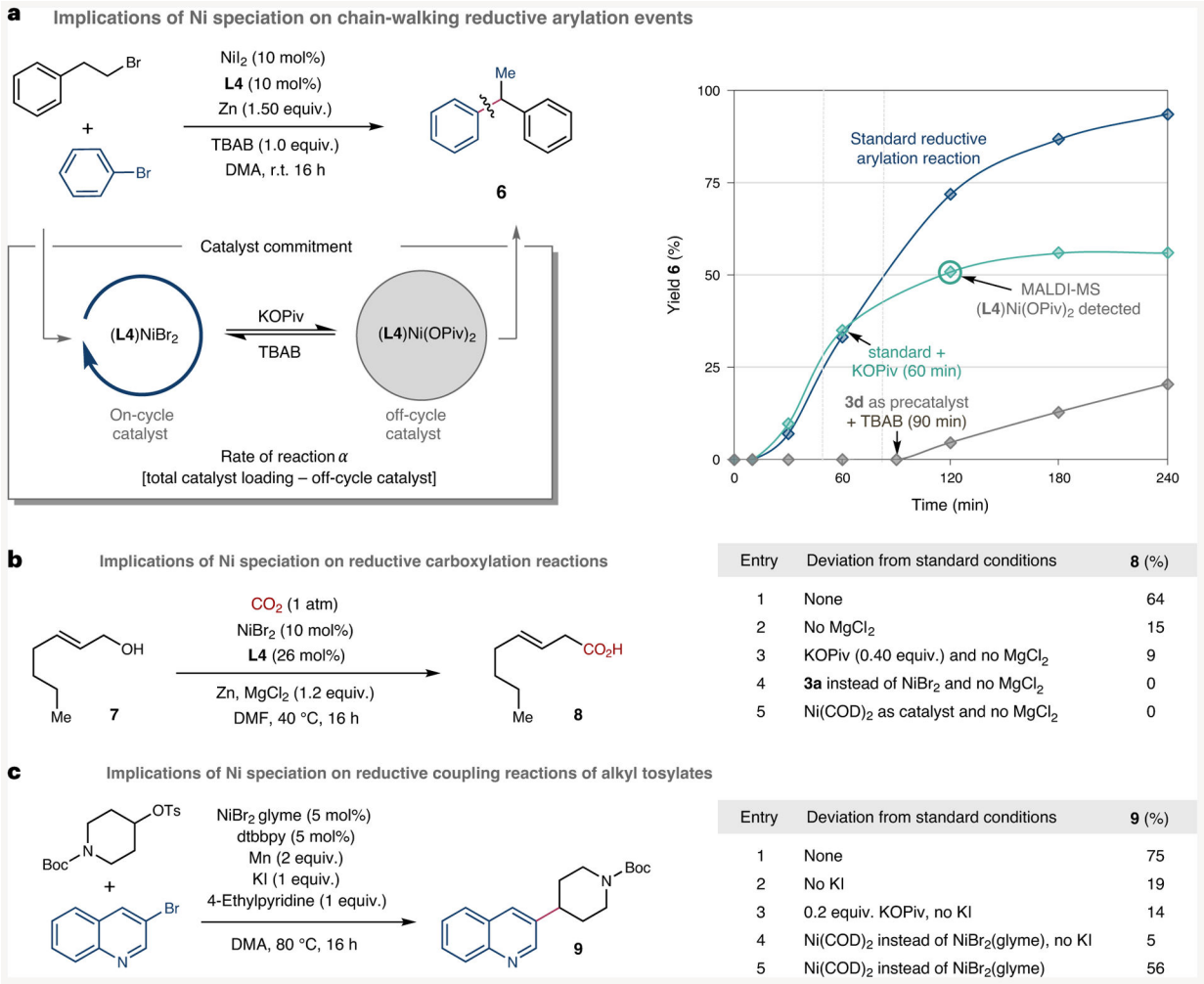

Entry	Deviation from standard conditions	8 (%)
1	None	64
2	No $MgCl_2$	15
3	KOPiv (0.40 equiv.) and no $MgCl_2$	9
4	**3a** instead of $NiBr_2$ and no $MgCl_2$	0
5	$Ni(COD)_2$ as catalyst and no $MgCl_2$	0

Entry	Deviation from standard conditions	9 (%)
1	None	75
2	No KI	19
3	0.2 equiv. KOPiv, no KI	14
4	$Ni(COD)_2$ instead of $NiBr_2$(glyme), no KI	5
5	$Ni(COD)_2$ instead of $NiBr_2$(glyme)	56

Fig. 6 |. Catalytic relevance of electron transfer.

a, Monitoring chain-walking reductive coupling reactions, with added potassium pivalate (0.4 equiv.) or using (**L4**)Ni(OPiv)$_2$ (**3a**) as a precatalyst. Blue trace, standard catalytic conditions; teal trace, standard catalytic conditions with KOPiv added after 60 minutes; grey trace, modified reaction conditions using **3d** as a precatalyst and without TBAB until it is added after 90 minutes. **b**, Implications of Ni speciation on Ni-catalysed reductive carboxylation reactions in the presence of exogenous organic bases or in the absence of halide salts. The tables describe deviations from the standard reductive carboxylation reaction conditions with the yield of the corresponding carboxylic acid. **c**, Implications of Ni speciation of Ni-catalysed reductive coupling reactions of alkyl tosylates. The table describes deviations from the standard reductive coupling reaction conditions with the yield of the corresponding cross-coupled product. TBAB, tetrabutyl ammonium bromide; r.t., room temperature; COD, cyclooctadiene; dtbbpy, 4,4’-di-*tert*-butyl-2,2’-dipyridyl; Ts = tosyl; Boc = tert-butyloxycarbonyl; DMA = dimethylacetamide; DMF = dimethylformamide; TBAB = tetrabutylammonium bromide.